Test of the flavour independence of α_s

D. Buskulic, D. Casper, I. de Bonis, D. Decamp, P. Ghez, C. Goy, J.P. Lees, M.N. Minard, P. Odier, B. Pietrzyk, et al.

EUROPEAN ORGANIZATION FOR NUCLEAR RESEARCH

CERN-PPE/95-018
21 February 1995

Test of the Flavour Independence of α_s

The ALEPH Collaboration*

Abstract

Using about 950 000 hadronic events collected during 1991 and 1992 with the ALEPH detector, the ratios $r^b = \alpha_s^b/\alpha_s^{udsc}$ and $r^{uds} = \alpha_s^{uds}/\alpha_s^{cb}$ have been measured in order to test the flavour independence of the strong coupling constant α_s. The analysis is based on event–shape variables using the full hadronic sample, two b-quark samples enriched by lepton tagging and lifetime tagging, and a light-quark sample enriched by lifetime antitagging. The combined results are $r^b = 1.002 \pm 0.023$ and $r^{uds} = 0.971 \pm 0.023$.

(Submitted to Phys. Lett. B)

*See the following pages for the list of authors.

The ALEPH Collaboration

D. Buskulic, D. Casper, I. De Bonis, D. Decamp, P. Ghez, C. Goy, J.-P. Lees, M.-N. Minard, P. Odier, B. Pietrzyk

Laboratoire de Physique des Particules (LAPP), IN^{2}P^3-CNRS, 74019 Annecy-le-Vieux Cedex, France

F. Ariztizabal, M. Chmeissani, J.M. Crespo, I. Efthymiopoulos, E. Fernandez, M. Fernandez-Bosman, V. Gaitan, Ll. Garrido,[15] M. Martinez, S. Orteu, A. Pacheco, C. Padilla, F. Palla, A. Pascual, J.A. Perlas, F. Sanchez, F. Teubert

Institut de Fisica d'Altes Energies, Universitat Autonoma de Barcelona, 08193 Bellaterra (Barcelona), Spain[7]

D. Creanza, M. de Palma, A. Farilla, G. Iaselli, G. Maggi,[3] N. Marinelli, S. Natali, S. Nuzzo, A. Ranieri, G. Raso, F. Romano, F. Ruggieri, G. Selvaggi, L. Silvestris, P. Tempesta, G. Zito

Dipartimento di Fisica, INFN Sezione di Bari, 70126 Bari, Italy

X. Huang, J. Lin, Q. Ouyang, T. Wang, Y. Xie, R. Xu, S. Xue, J. Zhang, L. Zhang, W. Zhao

Institute of High-Energy Physics, Academia Sinica, Beijing, The People's Republic of China[8]

G. Bonvicini, M. Cattaneo, P. Comas, P. Coyle, H. Drevermann, A. Engelhardt, R.W. Forty, M. Frank, M. Girone, R. Hagelberg, J. Harvey, R. Jacobsen,[24] P. Janot, B. Jost, J. Knobloch, I. Lehraus, M. Maggi, C. Markou,[27] E.B. Martin, P. Mato, H. Meinhard, A. Minten, R. Miquel, T. Oest, P. Palazzi, J.R. Pater, P. Perrodo, J.-F. Pusztaszeri, F. Ranjard, P. Rensing, L. Rolandi, D. Schlatter, M. Schmelling, O. Schneider, W. Tejessy, I.R. Tomalin, A. Venturi, H. Wachsmuth, W. Wiedenmann, T. Wildish, W. Witzeling, J. Wotschack

European Laboratory for Particle Physics (CERN), 1211 Geneva 23, Switzerland

Z. Ajaltouni, M. Bardadin-Otwinowska,[2] A. Barres, C. Boyer, A. Falvard, P. Gay, C. Guicheney, P. Henrard, J. Jousset, B. Michel, S. Monteil, J-C. Montret, D. Pallin, P. Perret, F. Podlyski, J. Proriol, J.-M. Rossignol, F. Saadi

Laboratoire de Physique Corpusculaire, Université Blaise Pascal, IN^{2}P^3-CNRS, Clermont-Ferrand, 63177 Aubière, France

T. Fearnley, J.B. Hansen, J.D. Hansen, J.R. Hansen, P.H. Hansen, B.S. Nilsson

Niels Bohr Institute, 2100 Copenhagen, Denmark[9]

A. Kyriakis, E. Simopoulou, I. Siotis, A. Vayaki, K. Zachariadou

Nuclear Research Center Demokritos (NRCD), Athens, Greece

A. Blondel,[21] G. Bonneaud, J.C. Brient, P. Bourdon, L. Passalacqua, A. Rougé, M. Rumpf, R. Tanaka, A. Valassi, M. Verderi, H. Videau

Laboratoire de Physique Nucléaire et des Hautes Energies, Ecole Polytechnique, IN^{2}P^3-CNRS, 91128 Palaiseau Cedex, France

D.J. Candlin, M.I. Parsons

Department of Physics, University of Edinburgh, Edinburgh EH9 3JZ, United Kingdom[10]

E. Focardi, G. Parrini

Dipartimento di Fisica, Università di Firenze, INFN Sezione di Firenze, 50125 Firenze, Italy

M. Corden, M. Delfino,[12] C. Georgiopoulos, D.E. Jaffe

Supercomputer Computations Research Institute, Florida State University, Tallahassee, FL 32306-4052, USA [13,14]

A. Antonelli, G. Bencivenni, G. Bologna,[4] F. Bossi, P. Campana, G. Capon, F. Cerutti, V. Chiarella, G. Felici, P. Laurelli, G. Mannocchi,[5] F. Murtas, G.P. Murtas, M. Pepe-Altarelli

Laboratori Nazionali dell'INFN (LNF-INFN), 00044 Frascati, Italy

S.J. Dorris, A.W. Halley, I. ten Have,[6] I.G. Knowles, J.G. Lynch, W.T. Morton, V. O'Shea, C. Raine, P. Reeves, J.M. Scarr, K. Smith, M.G. Smith, A.S. Thompson, F. Thomson, S. Thorn, R.M. Turnbull

Department of Physics and Astronomy, University of Glasgow, Glasgow G12 8QQ,United Kingdom[10]

U. Becker, O. Braun, C. Geweniger, G. Graefe, P. Hanke, V. Hepp, E.E. Kluge, A. Putzer, B. Rensch, M. Schmidt, J. Sommer, H. Stenzel, K. Tittel, S. Werner, M. Wunsch

Institut für Hochenergiephysik, Universität Heidelberg, 69120 Heidelberg, Fed. Rep. of Germany[16]

R. Beuselinck, D.M. Binnie, W. Cameron, D.J. Colling, P.J. Dornan, N. Konstantinidis, L. Moneta, A. Moutoussi, J. Nash, G. San Martin, J.K. Sedgbeer, A.M. Stacey

Department of Physics, Imperial College, London SW7 2BZ, United Kingdom[10]

G. Dissertori, P. Girtler, E. Kneringer, D. Kuhn, G. Rudolph

Institut für Experimentalphysik, Universität Innsbruck, 6020 Innsbruck, Austria[18]

C.K. Bowdery, T.J. Brodbeck, P. Colrain, G. Crawford, A.J. Finch, F. Foster, G. Hughes, T. Sloan, E.P. Whelan, M.I. Williams

Department of Physics, University of Lancaster, Lancaster LA1 4YB, United Kingdom[10]

A. Galla, A.M. Greene, K. Kleinknecht, G. Quast, J. Raab, B. Renk, H.-G. Sander, R. Wanke, C. Zeitnitz

Institut für Physik, Universität Mainz, 55099 Mainz, Fed. Rep. of Germany[16]

J.J. Aubert, A.M. Bencheikh, C. Benchouk, A. Bonissent, G. Bujosa, D. Calvet, J. Carr, C. Diaconu, F. Etienne, M. Thulasidas, D. Nicod, P. Payre, D. Rousseau, M. Talby

Centre de Physique des Particules, Faculté des Sciences de Luminy, IN^{2}P^3-CNRS, 13288 Marseille, France

I. Abt, R. Assmann, C. Bauer, W. Blum, D. Brown,[24] H. Dietl, F. Dydak,[21] C. Gotzhein, K. Jakobs, H. Kroha, G. Lütjens, G. Lutz, W. Männer, H.-G. Moser, R. Richter, A. Rosado-Schlosser, A.S. Schwarz,[23] R. Settles, H. Seywerd, U. Stierlin,[2] R. St. Denis, G. Wolf

Max-Planck-Institut für Physik, Werner-Heisenberg-Institut, 80805 München, Fed. Rep. of Germany[16]

R. Alemany, J. Boucrot, O. Callot, A. Cordier, F. Courault, M. Davier, L. Duflot, J.-F. Grivaz, Ph. Heusse, M. Jacquet, D.W. Kim,[19] F. Le Diberder, J. Lefrançois, A.-M. Lutz, G. Musolino, I. Nikolic, H.J. Park, I.C. Park, M.-H. Schune, S. Simion, J.-J. Veillet, I. Videau

Laboratoire de l'Accélérateur Linéaire, Université de Paris-Sud, IN^{2}P^3-CNRS, 91405 Orsay Cedex, France

D. Abbaneo, P. Azzurri, G. Bagliesi, G. Batignani, S. Bettarini, C. Bozzi, G. Calderini, M. Carpinelli, M.A. Ciocci, V. Ciulli, R. Dell'Orso, I. Ferrante, L. Foà,[1] F. Forti, A. Giassi, M.A. Giorgi, A. Gregorio, F. Ligabue, A. Lusiani, P.S. Marrocchesi, A. Messineo, G. Rizzo, G. Sanguinetti, A. Sciabà, P. Spagnolo, J. Steinberger, R. Tenchini, G. Tonelli,[26] G. Triggiani, C. Vannini, P.G. Verdini, J. Walsh

Dipartimento di Fisica dell'Università, INFN Sezione di Pisa, e Scuola Normale Superiore, 56010 Pisa, Italy

A.P. Betteridge, G.A. Blair, L.M. Bryant, Y. Gao, M.G. Green, D.L. Johnson, T. Medcalf, Ll.M. Mir, J.A. Strong

Department of Physics, Royal Holloway & Bedford New College, University of London, Surrey TW20 OEX, United Kingdom[10]

V. Bertin, D.R. Botterill, R.W. Clifft, T.R. Edgecock, S. Haywood, M. Edwards, P. Maley, P.R. Norton, J.C. Thompson

Particle Physics Dept., Rutherford Appleton Laboratory, Chilton, Didcot, Oxon OX11 OQX, United Kingdom[10]

B. Bloch-Devaux, P. Colas, H. Duarte, S. Emery, W. Kozanecki, E. Lançon, M.C. Lemaire, E. Locci, B. Marx, P. Perez, J. Rander, J.-F. Renardy, A. Rosowsky, A. Roussarie, J.-P. Schuller, J. Schwindling, D. Si Mohand, A. Trabelsi, B. Vallage

CEA, DAPNIA/Service de Physique des Particules, CE-Saclay, 91191 Gif-sur-Yvette Cedex, France[17]

R.P. Johnson, H.Y. Kim, A.M. Litke, M.A. McNeil, G. Taylor

Institute for Particle Physics, University of California at Santa Cruz, Santa Cruz, CA 95064, USA[22]

A. Beddall, C.N. Booth, R. Boswell, S. Cartwright, F. Combley, I. Dawson, A. Koksal, M. Letho, W.M. Newton, C. Rankin, L.F. Thompson

Department of Physics, University of Sheffield, Sheffield S3 7RH, United Kingdom[10]

A. Böhrer, S. Brandt, G. Cowan, E. Feigl, C. Grupen, G. Lutters, J. Minguet-Rodriguez, F. Rivera,[25] P. Saraiva, L. Smolik, F. Stephan

Fachbereich Physik, Universität Siegen, 57068 Siegen, Fed. Rep. of Germany[16]

L. Bosisio, R. Della Marina, G. Ganis, G. Giannini, B. Gobbo, L. Pitis, F. Ragusa[20]

Dipartimento di Fisica, Università di Trieste e INFN Sezione di Trieste, 34127 Trieste, Italy

J. Rothberg, S. Wasserbaech

Experimental Elementary Particle Physics, University of Washington, WA 98195 Seattle, U.S.A.

S.R. Armstrong, L. Bellantoni, P. Elmer, Z. Feng, D.P.S. Ferguson, Y.S. Gao, S. González, J. Grahl, J.L. Harton, O.J. Hayes, H. Hu, P.A. McNamara III, J.M. Nachtman, W. Orejudos, Y.B. Pan, Y. Saadi, M. Schmitt, I.J. Scott, V. Sharma, J.D. Turk, A.M. Walsh, F.V. Weber,[1] Sau Lan Wu, X. Wu, J.M. Yamartino, M. Zheng, G. Zobernig

Department of Physics, University of Wisconsin, Madison, WI 53706, USA[11]

[1]Now at CERN, 1211 Geneva 23, Switzerland.
[2]Deceased.
[3]Now at Dipartimento di Fisica, Università di Lecce, 73100 Lecce, Italy.
[4]Also Istituto di Fisica Generale, Università di Torino, Torino, Italy.
[5]Also Istituto di Cosmo-Geofisica del C.N.R., Torino, Italy.
[6]Now at TSM Business School, Enschede, The Netherlands.
[7]Supported by CICYT, Spain.
[8]Supported by the National Science Foundation of China.
[9]Supported by the Danish Natural Science Research Council.
[10]Supported by the UK Particle Physics and Astronomy Research Council.
[11]Supported by the US Department of Energy, contract DE-AC02-76ER00881.
[12]On leave from Universitat Autonoma de Barcelona, Barcelona, Spain.
[13]Supported by the US Department of Energy, contract DE-FG05-92ER40742.
[14]Supported by the US Department of Energy, contract DE-FC05-85ER250000.
[15]Permanent address: Universitat de Barcelona, 08208 Barcelona, Spain.
[16]Supported by the Bundesministerium für Forschung und Technologie, Fed. Rep. of Germany.
[17]Supported by the Direction des Sciences de la Matière, C.E.A.
[18]Supported by Fonds zur Förderung der wissenschaftlichen Forschung, Austria.
[19]Permanent address: Kangnung National University, Kangnung, Korea.
[20]Now at Dipartimento di Fisica, Università di Milano, Milano, Italy.
[21]Also at CERN, 1211 Geneva 23, Switzerland.
[22]Supported by the US Department of Energy, grant DE-FG03-92ER40689.
[23]Now at DESY, Hamburg, Germany.
[24]Now at Lawrence Berkeley Laboratory, Berkeley, CA 94720, USA.
[25]Partially supported by Colciencias, Colombia.
[26]Also at Istituto di Matematica e Fisica, Università di Sassari, Sassari, Italy.
[27]Now at University of Athens, 157-71 Athens, Greece.

1 Introduction

An important property of QCD is the flavour independence of the strong coupling constant α_s. The experimental results from the quarkonium states[1] and from the bottom production at $p\bar{p}$ colliders[2] are consistent with the flavour independence. Also the relative coupling strengths for charm and bottom quarks have been measured in e^+e^- colliders at center of mass energies around 30 GeV[3] and support the flavour independence within large uncertainties. Results at Z energies were published recently[4, 5].

The method used in this analysis has been already employed to measure α_s at the Z pole[6]. It consists of comparing event–shape–variable distributions for hadronic events with the QCD predictions calculated to second order[7]. The flavour independence is tested by comparing two heavy-flavour samples, one enriched by lepton tag and one by lifetime tag, and a light-flavour sample enriched by lifetime antitag, to the full sample of hadronic events, from which $r^b = \alpha_s^b/\alpha_s^{udsc}$ and $r^{uds} = \alpha_s^{uds}/\alpha_s^{cb}$ are determined.

2 Event selection and data analysis

The ALEPH detector, which provides both tracking information and calorimetry over almost the full solid angle, is described elsewhere[8, 9]. Charged tracks are measured by a vertex detector (VDET), a drift chamber (ITC) and by a large time projection chamber (TPC) immersed in a 1.5 T magnetic field. The TPC provides up to 338 measurements of the specific ionization, $\mathrm{d}E/\mathrm{d}x$, of each charged track. The full tracking system allows the measurement of the momentum of charged particles with a resolution of $\sigma(p_T)/p_T = 6 \cdot 10^{-4}(\mathrm{GeV}/c)^{-1} p \oplus 5 \cdot 10^{-3}$ and the impact parameter δ of the charged tracks with a resolution of $\sigma(\delta) = 25\mu\mathrm{m} + 95(\mu\mathrm{mGeV}/c)/p$[9].

The tracking system is surrounded by the electromagnetic calorimeter (ECAL), which is constructed of 45 layers of lead interleaved with proportional wire chambers. The ECAL has an energy resolution of $\sigma(E)/E = 0.178(\mathrm{GeV})^{\frac{1}{2}}/\sqrt{E} \oplus 0.019$ and is used together with the $\mathrm{d}E/\mathrm{d}x$ measurements of the TPC to identify electrons. The hadron calorimeter (HCAL) consists of the iron of the magnet return yoke interleaved with 23 layers of streamer tubes. The HCAL is surrounded by two layers of muon chambers that are used in conjunction with the HCAL and the tracking detectors to identify muons. Both charged tracks and neutral particles are used, via the energy flow reconstruction algorithm described in Ref.[9], in the performed analyses.

Two different data analyses have been performed. The first is based on the selection of a hadronic sample ($\mathrm{Q\bar{Q}}1$) where at least 5 good tracks reconstructed by the TPC in an event are required. A track is defined as "good" when the angle with respect to the beam axis is greater then 18.2°, there are at least 4 TPC points used in the fit of the track, and it passes through a cylinder centered around the fitted average beam position, with a radius of 2 cm and a length of 10 cm. In order to remove two–photon events and beam–gas interactions the sum of the momenta of all tracks must be greater than 10% of the center of mass energy. The background is $(0.7 \pm 0.1)\%$ coming from τ pairs and

two–photon interactions. The total efficiency of this selection is 97.4%[10]. After these cuts about 950 000 hadronic events collected during 1991 and 1992 remain.

From this hadronic sample a first b-enriched sample (BTAG1) is selected by requiring a prompt electron or muon candidate. The lepton tagging is described in detail in Ref.[11]. The momentum of the lepton must be greater then 3 GeV/c and the transverse momentum with respect to the nearest jet must be greater then 1.25 GeV/c. With these cuts the BTAG1 sample contains about 40 000 events. The b-purity $f^b_{\mathrm{BTAG1}} = 88\%$, as has been estimated by Monte Carlo using the results of Ref.[11].

The second analysis was performed in order to complement the first one and to extend the analysis to measure also the ratio r^{uds}. It is based on a slightly different selection of the hadronic sample ($\mathrm{Q\bar{Q}}2$) with more stringent cuts in order to reduce systematic errors. At least 6 good tracks are required, the charged energy should exceed 15 GeV and the total visible energy has to be greater then 45 GeV. The selection efficiency is 91% and the sample consists of about 900 000 events.

Starting from the $\mathrm{Q\bar{Q}}2$ sample a second b-enriched sample (BTAG2) and a light-quark-enriched sample (UDSTAG) are selected using lifetime information. The precise impact parameter measurements of the charged tracks are used to determine the confidence level P_{vtag} that all the tracks originate from the primary vertex, as described in Ref.[12]. The UDSTAG sample of 300 000 events is selected by requiring $P_{vtag} > 0.18$ giving an uds-purity of $f^{uds}_{\mathrm{UDSTAG}} = 81\%$. By requiring $P_{vtag} < 0.0035$ the BTAG2 sample of 120 000 events is selected with a b-purity $f^b_{\mathrm{BTAG2}} = 86\%$.

In the following, $\mathfrak{S}$ stands for any selected sample, one of the two hadronic samples $\mathrm{Q\bar{Q}}1$ and $\mathrm{Q\bar{Q}}2$ or one of the three tagged samples BTAG1, UDSTAG and BTAG2. Each sample is composed of the quarks q to be tagged, where $q = b$ for $\mathfrak{S} \in \{\mathrm{BTAG1}, \mathrm{BTAG2}\}$ and $q = uds$ for $\mathfrak{S} = \mathrm{UDSTAG}$, and of a background of the complementary quarks q', where $q' = udsc$ for $\mathfrak{S} \in \{\mathrm{BTAG1}, \mathrm{BTAG2}\}$ and $q' = cb$ for $\mathfrak{S} = \mathrm{UDSTAG}$. When referring to generic quark types the symbol q may stand for q or q'.

The event–shape variables Thrust, C–parameter and differential two–jet rate were studied in this analysis. Thrust is defined as $\mathrm{T} = \max\left(\sum_i |\boldsymbol{p_i} \cdot \boldsymbol{n}\ | / \sum_i |\boldsymbol{p_i}\ |\right)$ where the unit vector $\boldsymbol{n}$ is the thrust axis and $\boldsymbol{p_i}$ the momentum of each final state particle. The C–parameter is the quadratic invariant of the spherocity tensor $S_{ij} = \left(\sum_a p^i_a p^j_a / p_a\right) / \sum_a p_a$, given by $\mathrm{C} = 3\,(\lambda_1\lambda_2 + \lambda_2\lambda_3 + \lambda_3\lambda_1)$, with $\lambda_{i=1,2,3}$ the eigenvalues of S_{ij}. The differential two–jet rate has been computed with the Jade[13] (y^J_{ij}) and the Durham[14] (y^D_{ij}) metric for the phase–space distance between a pair of jets i and j, with energies E_i and E_j and opening angle θ_{ij}, $y^J_{ij} = 2E_iE_j(1-\cos\theta_{ij})/E^2_{vis}$ and $y^D_{ij} = 2\min(E^2_i, E^2_j)(1-\cos\theta_{ij})/E^2_{vis}$. Jets are formed in an iterative procedure, always combining the pair with the smallest y_{ij} into one jet. The procedure is iterated until only three jets are left at which point the smallest y_{ij} is Y_3.

In the $\mathrm{Q\bar{Q}}1$ and BTAG1 samples all four event–shape variables were analyzed: Thrust, C–parameter, differential two–jet rate $\mathrm{D}_2(\mathrm{Y}_3)$ with the Jade algorithm $\mathrm{D}_2(-\ln\mathrm{Y}_3)$ with the Durham algorithm. Figure 1 shows these distributions for the two samples. The $-\ln\mathrm{Y}_3$ (Durham) plot clearly shows the b-mass effects in the fragmentation region ($-\ln\mathrm{Y}_3 > 4$), which is not used in the analysis. In the $\mathrm{Q\bar{Q}}2$, UDSTAG and BTAG2

samples the differential two-jet rates $D_2(Y_3)$ with Jade and Durham algorithms are studied. Figure 2 shows the distributions obtained in those cases.

A sample of 2.6 million simulated hadronic events was also analyzed. The Monte Carlo generator used is based on JETSET 7.3[15], with updated branching ratios. The initial state radiation (ISR) is simulated by the DYMU3 generator[16]. The light quark fragmentation and QCD parameters were optimized to fit the ALEPH data[17]. For heavy quarks, the Peterson fragmentation function is used[18], with the value of the fragmentation parameter for the b quark $\varepsilon_b = (3.2 \pm 1.7) \cdot 10^{-3}$[11]. The full sample of Monte Carlo events were processed through a detailed simulation of the ALEPH detector and the standard ALEPH reconstruction program.

3 Theoretical prediction and correction procedure

The QCD prediction to second order for a given event–shape variable X can be parameterized in the form[7]:

$$\frac{1}{\sigma_0}\frac{\mathrm{d}\sigma}{\mathrm{d}X} = \frac{\alpha_s(\mu^2)}{2\pi}A(X) + \left(\frac{\alpha_s(\mu^2)}{2\pi}\right)^2 \left(A(X)2\pi \mathrm{b}_0 \ \ln\frac{\mu^2}{\mathrm{M}_\mathrm{Z}^2} + B(X)\right) \ .$$

In the analysis described in this letter the theoretical expression was fit to the data at the renormalization scale $\mu^2 = 0.05 \cdot \mathrm{M}_\mathrm{Z}^2$, which was chosen to symmetrize the scale uncertainty. The resulting value of the strong coupling constant is translated to $\alpha_s(\mathrm{M}_\mathrm{Z}^2)$ using the two–loop expression:

$$\alpha_s(\mathrm{M}_\mathrm{Z}^2) = \frac{\alpha_s(\mu^2)}{\omega}\left(1 - \frac{\mathrm{b}_1}{\mathrm{b}_0}\frac{\alpha_s(\mu^2)}{\omega}\cdot\ln\omega\right) \ ,$$

where $\omega = 1 - \mathrm{b}_0\alpha_s(\mu^2)\ln(\mu^2/\mathrm{M}_\mathrm{Z}^2)$, $\mathrm{b}_0 = (33-2n_f)/12\pi$, and $\mathrm{b}_1 = (153-19n_f)/24\pi^2$, with the number of active flavours set to $n_f = 5$.

The coefficients $A(X)$ and $B(X)$ are computed for massless partons. Therefore mass corrections are needed in order to compare the theoretical prediction to the data. Corrections to the theoretical formulae are also computed to take into account hadronization and ISR using several Monte Carlo samples. The effects of the selection cuts and resolution of the detector were taken into account with correction factors computed with the Monte Carlo events described in Sect. 2.

This procedure modifies the theory such that it can be compared directly with the uncorrected experimental distributions. This correction from the parton to the detector level goes in the opposite direction to the one usually applied (i.e. from the detector to the parton level) and was chosen since correction in the usual direction is more model dependent. The implicit assumption of flavour independence of α_s in the correction procedure is thus avoided, which would enter when correcting the data back to parton level because even the tagged samples are mixtures of different quark flavours.

The individual corrections were determined in the following way:

- The sample of Monte Carlo events described in Sect. 2 is used to extract the effect of the resolution of the detector in the form of a transition matrix $M^q_{det}(X_i, X_j)$, which is the probability that a given event–shape variable X with the value X_j at hadron level has the value X_i at detector level.

- The biases due to the selection cuts applied lead to corrections $V^{q,\mathfrak{S}}_{cut}$ that are obtained from the same sample of Monte Carlo events by dividing bin per bin the distributions before and after selection of $\mathfrak{S}$–type events.

- The QED corrections V^q_{QED} are computed dividing bin per bin the distributions obtained with ISR, as described by DYMU3, by those without ISR.

- The hadronization corrections V^q_{had} are estimated by dividing bin per bin the distributions of Monte Carlo events before and after hadronization. Four different models are used. Three of them are based on the string model as implemented in JETSET 7.3 with different parton evolution schemes: (1) The $\mathcal{O}(\alpha_s^2)$ matrix element (ME) model, where an experimental optimization has been applied in order to reproduce the observed 4-jet rate[17]. This model is important since the second order QCD prediction for α_s has been used for the theoretical prediction. (2) The Parton Shower (PS) model, in which the parton level is defined to be the end of the shower evolution before the cut-off scale $Q_0 \sim 1$ GeV. (3) The PS-model with the cut-off scale of the parton shower at 7.2 GeV, chosen in order to reproduce the mean parton multiplicity of the second order matrix element model. (4) The fourth model is the HERWIG 5.8[19] parton-shower models which uses a cluster hadronization scheme.

- Quark mass effects at LEP energies have been recently computed in Ref.[20] at tree level, i.e. without loop corrections, to $\mathcal{O}(\alpha_s)$ ($q\bar{q}g$ diagrams) and $\mathcal{O}(\alpha_s^2)$ ($q\bar{q}q\bar{q}$ and $q\bar{q}gg$ diagrams) accuracy. From this correction factors were derived as

$$V^q_{mass}(X) = \frac{\left.\frac{\mathrm{d}\sigma}{\mathrm{d}X}\right|_{m=m_q}}{\left.\frac{\mathrm{d}\sigma}{\mathrm{d}X}\right|_{m=0}} \ ,$$

  assuming the b-quark mass and the c-quark mass to be $m_b = 5 \pm 0.5$ GeV/c^2 and $m_c = 1.5 \pm 0.2$ GeV/c^2, respectively. The other quarks are taken to be massless ($V^{uds}_{mass} = 1$). The available $\mathcal{O}(\alpha_s^2)$-calculations are incomplete, since they contain no loop corrections to $q\bar{q}g$ final states. For Thrust and C–parameter this implies, that divergencies which to $\mathcal{O}(\alpha_s)$ are restricted to the phase space region of back-to-back partons occur in the region of interest. Only the two–jet rate remains finite over the phase space used in the analysis. Because of this the correction factors V^q_{mass} used in this analysis are based only on the $\mathcal{O}(\alpha_s)$ matrix elements[20]. However, the fact that the mass corrections are sizeable indicates that higher order corrections might be important, and although incomplete, the tree level calculation to $\mathcal{O}(\alpha_s^2)$ are gauge invariant and thus may be employed to estimate the theoretical uncertainties. The effects of the mass corrections for all event–shape variables are shown in Figs. 3 and 4.

With the full set of corrections the theoretical prediction for quarks of type q in a sample $\mathfrak{S}$ becomes:

$$G^{q,\mathfrak{S}}(X_i) = \sum_j M^q_{det}(X_i, X_j) \cdot V^{q,\mathfrak{S}}_{cut}(X_j) \cdot V^q_{QED}(X_j) \cdot V^q_{had}(X_j) \cdot F^q(X_j) \ ,$$

where

$$F^q(X_j) = \frac{\sigma^q_0}{\sigma^q_T} \cdot \left[\frac{\alpha^q_s(\mu^2)}{2\pi} A(X_j) \cdot V^q_{mass} + \left(\frac{\alpha^q_s(\mu^2)}{2\pi} \right)^2 \left(A(X_j) \cdot V^q_{mass} 2\pi \mathrm{b}_0 \ ln \frac{\mu^2}{\mathrm{M}^2_\mathrm{Z}} + B(X_j) \right) \right] \ ,$$

with σ^q_0 the Born-level cross section for massless quarks of type q and σ^q_T the total cross section including mass effects[21].

4 Determination of r^b and r^{uds}

In order to extract $r^b = \alpha^b_s / \alpha^{udsc}_s$ and $r^{uds} = \alpha^{uds}_s / \alpha^{cb}_s$ from each event–shape variable a χ^2-fit of the theoretical expression

$$R_{th}(X) = \frac{G^{q,tag} \cdot f^q_{tag} + G^{q',tag} \cdot (1 - f^q_{tag})}{G^{q,\mathrm{Q\bar{Q}}} \cdot f^q_{\mathrm{Q\bar{Q}}} + G^{q',\mathrm{Q\bar{Q}}} \cdot (1 - f^q_{\mathrm{Q\bar{Q}}})}$$

is performed to the measured ratio

$$R_{data} = \frac{\frac{1}{N}\frac{\mathrm{d}N}{\mathrm{d}X}\Big|_{tag}}{\frac{1}{N}\frac{\mathrm{d}N}{\mathrm{d}X}\Big|_{\mathrm{Q\bar{Q}}}}$$

of the normalized differential cross sections of the tagged sample and the inclusive hadronic sample. The fractions f^q_{tag} and $f^q_{\mathrm{Q\bar{Q}}}$, respectively, denote the purities of the tagged quark type q in the tagged and the corresponding untagged hadronic sample. The strong coupling constants α^q_s in G^q for the quarks of type q and $\alpha^{q'}_s$ in $G^{q'}$ for the complementary quarks are constrained such that the mean value is the global average 0.118 ± 0.007[22]. For each variable the fit range, shown in Tables 1 and 2, is chosen to minimize experimental corrections and theoretical uncertainties.

The central values for r^b and r^{uds} have been computed as the mean between the maximum and minimum values of the results obtained from the four hadronization models. The ME model and the parton shower model with $Q_0 = 7.2$ GeV give similar results, and so do the models based on the full parton shower evolution. Both groups differ significantly from each other (see uncertainty due to hadronization correction discussed below). The mean values are shown in Tables 1 and 2 together with the statistical errors that include the Monte Carlo statistical error. Figures 3 and 4 show the measured ratios R_{data} for each variable compared to the fitted theoretical predictions. The agreement is good and extends well outside the fit range.

Systematic effects

The systematic errors can be divided into two categories, linked to experimental and to theoretical uncertainties. The procedures used to determine those uncertainties are described below. The results for the measurements of r^b are listed in Table 1 and in Table 2 for the measurements of r^{uds}.

The effect of ε_b has been estimated by varying this parameter, by one standard deviation from the measured value, in the Monte Carlo.

The effect of the purities of the samples has been studied as follows. Since the values of R_{data} are near to 1.0 in the fit ranges, the measured r^b and r^{uds} are almost independent on the relative composition of the samples. The R_{data} has therefore been varied within the statistical errors and the maximum variation, obtained by varying the parameter f^q_{tag} by one standard deviation, has been kept as systematic error.

The fit range is varied by ± 1 bin and half of the maximum variation is taken as systematic error.

The selection cut biases were determined from Monte-Carlo simulations. The simulations are good to 10%, which is supported by comparing measured and simulated p and $p_\perp$ distributions of leptons with respect to the jet axis. Similarly, the lifetime tag performances on all hadronic events are reproduced by the Monte Carlo within 1%, which implies that the correction factors for the three-jet topologies analyzed here are correct to better than 10%. The systematic errors due to selection cut biases thus were determined, by varying the bias corrections by 10% of their deviation from unity. The resulting changes in r^b and r^{uds} were taken as a systematic error.

The simulation of the detector performances is precise within 10%. This uncertainty has been propagated to the final result. The full analysis has been also done with only charged tracks giving results which are compatible within statistics.

The systematic error coming from the inclusive $\alpha_s(\mathrm{M}_\mathrm{Z}^2)$ has been estimated by varying it within the quoted uncertainties.

The impact of perturbative higher order contributions is inferred by varying the renormalization scale μ from the b–quark mass to the Z mass.

The uncertainty due to hadronization corrections has been estimated using the results based on the four Monte Carlo models. The uncertainty has been taken to be half of the maximum variation of the fit results obtained from the different models.

The uncertainty due to the masses of the b- and c–quark mass has been determined by varying the value assumed in the mass corrections. The uncertainties of the quark masses were assumed to be 100% correlated.

To estimate the uncertainties due to the mass corrections the tree level second order mass calculations are used. For the jet-rates, where the tree-level calculation are finite, the differences between the results obtained with the first order and the second order mass corrections are taken as systematic error. Assuming that the impact of the second order correction is proportional to the one of the first order mass correction, the respective uncertainties for Thrust and C–parameter are estimated by correspondingly scaling the larger of the errors found for the jet rates.

5 Combined results

In order to combine the results coming from the different studies the statistical correlation matrix has been extracted from the data. The data has been divided in 21 sub-samples, and r^b and r^{uds} have been determined from each sample for all the event–shape variables.

The covariance matrix for the systematic error is given by the sum of covariance matrices for all individual systematic sources, and is constructed in the following way: The errors due to the choice of the fit range are assumed independent. The errors on the purity of the samples and on the bias of the selections are uncorrelated for variables studied with different tag methods. All other uncertainties are taken to be correlated such, that the covariance of two measurements is defined to be the minimum squared of the errors on the single measurements. This ansatz implies that the variable with larger error has no information that is not already contained in the variable with the smaller error.

In Table 3 the correlation coefficients computed from the statistical and systematic covariance matrices of all the measurements of r^b are shown. The total correlation of the two measurements of r^{uds} is 68%. These lead to the measurement of r^b to be

$$r^b = 1.002 \pm 0.009(stat.) \pm 0.005(syst.) \pm 0.021(theo.)$$

and the measurements of r^{uds} to be

$$r^{uds} = 0.971 \pm 0.009(stat.) \pm 0.011(syst.) \pm 0.018(theo.) \ .$$

The central value in both cases is the weighted average of the individual results, with the weights proportional to $1/\sigma^2_{tot}$ where σ_{tot} is the statistical and systematic error combined in quadrature. The correlations only affect the error estimate for the average.

In Ref.[5], a procedure has been followed which results in a smaller systematic error. The main differences are that, here, the renormalization scale range was varied over a larger range and errors due to hadronization and mass effects were estimated in a more conservative way. The ME Monte Carlo has been included to estimate hadronization corrections for reasons given above, while in Ref.[5] it was not used. Also, that analysis did not use the available second-order tree level calculation to estimate the uncertainties due to mass effect. If a similar procedure were used here, the theoretical uncertainties would decrease to ± 0.010 and ± 0.011 for r^b and r^{uds} respectively. The more conservative assessment of the theoretical uncertainties, essentially consistent with Ref.[6], was chosen, because calculations at 3^{rd} order QCD and a complete $\mathcal{O}(\alpha_s^2)$ treatment of mass effect are still missing.

6 Conclusions

The ratio of the strong coupling constants for b-quarks and light quarks, $r^b = \alpha_s^b/\alpha_s^{udsc}$, was measured selecting two enriched samples of $b\bar{b}$ events, one with a high $p_\perp$ lepton

and one with lifetime information. The lifetime information has been used to select an enriched sample of light quarks to measure $r^{uds} = \alpha_s^{uds}/\alpha_s^{cb}$. The analyses are based on event–shape variables. Thrust, C–parameter and Differential two–jet rates computed with the Jade and Durham algorithms are used in the lepton tag study. Results from the lifetime tag come from the differential two jet rates.

The combined results $r^b = 1.002 \pm 0.023$ and $r^{uds} = 0.971 \pm 0.023$ are consistent with the flavour independence of the strong coupling constant.

Acknowledgement

We wish to congratulate our colleagues in the CERN accelerator divisions for the successful operation of LEP. We are grateful to the engineers and technicians in all our institutions for their contribution towards ALEPH's success. We thank A. Ballestrero,E. Maina and S. Moretti for useful discussions. Those of us from non-member countries thank CERN for its hospitality.

References

[1] R.D. Schamberger et al., (CUSB collab.) Phys. Lett. B 138 (1984) 225.
S.E. Csorna et al., (CLEO collab.) Phys. Rev. Lett. 56 (1986) 1222.
H. Albrecht et al., (ARGUS collab.) Phys. Lett. B 199 (1987) 291.
W. Kwong et al., Phys. Rev. D 37 (1988) 3210.

[2] A. Geiser, (UA1 collab.) Proc. of the 27^{th} Rencontre de Moriond: QCD and High Energy Hadronic Interaction, Les Arcs, France, ed. J. Tran Tranh Van (Editions Frontieres) (1992) 159.

[3] W. Braunschweig et al., (TASSO collab.) Z. Phys. C 44 (1989) 365.

[4] B. Adeva et al., (L3 collab.) Phys. Lett. B 271 (1991) 461.
R. Akers et al., (OPAL collab.) Z. Phys. C 60 (1993) 397.
P. Albreu et al., (DELPHI collab.) Phys. Lett. B 307 (1993) 221.
K. Abe et al., (SLD collab.) SLAC-pub-6687 (1994).

[5] R. Akers et al., (OPAL collab.) "Determination of event shape distributions and α_s^b from $Z \to b\bar{b}$ at LEP" CERN-PPE/94-123.

[6] D. Decamp et al., (ALEPH collab.) Phys. Lett. B 255 (1991) 623.

[7] Z. Kunszt et al., Proc. Workshop on Z Physics at LEP, eds. G. Altarelli, R. Kleiss and G. Verzegnassi, CERN Report 89–08 vol.I, p.373 ff.

[8] D. Decamp et al., (ALEPH collab.) Nucl. Instr. Meth. A 294 (1990) 121;

[9] D. Buskulic et al., (ALEPH collab.) "Performance of the ALEPH detector at LEP" CERN-PPE/94-170.

[10] D. Decamp et al., (ALEPH collab.) Z. Phys. C 53 (1992) 1.

[11] D. Buskulic et al., (ALEPH collab.) Z. Phys. C 62 (1994) 441.

[12] D. Buskulic et al., (ALEPH collab.) Phys. Lett. B 313 (1993) 535.

[13] W. Bartel et al., (Jade collab.) Z. Phys. C 33 (1986) 23.
W. Bartel et al., (Jade collab.) Phys. Lett. B 213 (1988) 235.

[14] S. Catani et al., Phys. Lett. B 269 (1991) 432.
Durham Workshop, W. J. Stirling, J. Phys. G 17 (1991) 1657.

[15] T. Sjöstrand and M. Bengtsson, Computer Phys. Commun. 43 (1987) 367.

[16] J.E. Campagne and R. Zitoun, "An expression of the electron structure function in QED" LPNHE 88-06.
J.E. Campagne and R. Zitoun, Z. Phys. C 43 (1989) 469.
R. Kleiss et al., Proc. Workshop on Z Physics at LEP, eds. G. Altarelli, R. Kleiss and G. Verzegnassi, CERN Report 89–08 vol.III, pag.41 ff.

[17] D. Buskulic et al., (ALEPH collab.) Z. Phys. C 55 (1992) 209.

[18] C. Peterson et al., Phys. Rev. D 27 (1983) 105.

[19] G. Marchesini and B.R. Webber, Nucl. Phys. B310 (1988) 461.
G. Marchesini et al., Comp. Phys. Comm. 67 (1992) 465.

[20] A. Ballestrero et al., Phys. Lett. B 294 (1992) 425 and private communications.

[21] T. Hebbeker, "QCD correction to Γ_{had}" PITHA 91/08; Phys. Rep. 217 (1992) 69.

[22] S. Bethke, Proc. of the XXVI International Conference on High Energy Physics, Dallas, Texas, ed. J. Sanford (AIP Conference Proceedings No.272) (1992) 81.

	lepton tag				lifetime tag	
	Thrust	C–param.	$Y_3(\text{Jade})$	$-\ln Y_3(\text{Durham})$	$Y_3(\text{Jade})$	$Y_3(\text{Durham})$
	Fit range					
low end	0.75	0.50	0.07	1.6	0.07	0.03
high end	0.90	0.74	0.23	3.2	0.23	0.17
r^b	0.993	0.969	1.027	1.014	1.024	1.033
Stat. err.	± 0.011	± 0.013	± 0.014	± 0.014	± 0.008	± 0.009
Exp. err. source	Δr^b					
ε_b	± 0.001	± 0.001	± 0.004	± 0.006	± 0.009	± 0.008
purity	± 0.002	± 0.002	± 0.002	± 0.003	± 0.002	± 0.003
fit range	± 0.003	± 0.003	± 0.002	± 0.003	± 0.002	± 0.005
tagging bias	± 0.002	± 0.002	± 0.001	± 0.001	± 0.012	± 0.015
det. simulation	± 0.002	± 0.002	± 0.002	± 0.002	± 0.002	± 0.002
Theor. err. source	Δr^b					
$\alpha_s(M_Z^2)$	± 0.001	± 0.001	± 0.002	± 0.002	± 0.002	± 0.002
ren. scale	± 0.004	± 0.003	± 0.014	± 0.013	± 0.012	± 0.014
hadronization	± 0.008	± 0.010	± 0.018	± 0.018	± 0.022	± 0.016
quark masses	± 0.003	± 0.004	± 0.005	± 0.006	± 0.005	± 0.008
mass correction	± 0.016	± 0.016	± 0.021	± 0.017	± 0.021	± 0.011
Syst. err.	± 0.019	± 0.020	± 0.032	± 0.030	± 0.037	± 0.031

Table 1: Results on the determination of r^b for each method used. The total systematic errors are the quadratic sum of the individual contributions.

	$Y_3(\text{Jade})$	$Y_3(\text{Durham})$
	Fit range	
low end	0.07	0.03
high end	0.23	0.17
r^{uds}	0.974	0.968
Stat. err.	± 0.011	± 0.012
Exp. err. source	Δr^{uds}	
ε_b	± 0.006	± 0.004
purity	± 0.007	± 0.008
fit range	± 0.002	± 0.004
tagging bias	± 0.006	± 0.007
det. simulation	± 0.001	± 0.001
Theor. err. source	Δr^{uds}	
$\alpha_s(M_Z^2)$	± 0.002	± 0.002
ren. scale	± 0.008	± 0.008
hadronization	± 0.012	± 0.013
quark masses	± 0.004	± 0.005
mass correction	± 0.014	± 0.008
Syst. err.	± 0.023	± 0.022

Table 2: Results on the determination of r^{uds} from the lifetime analysis. The total systematic errors are the quadratic sum of the individual contributions.

Variable	Method	Total correlation coefficients					
Thrust	lepton tag	1	0.87	0.63	0.62	0.42	0.30
C–param.	lepton tag		1	0.62	0.69	0.43	0.33
$Y_3(\text{Jade})$	lepton tag			1	0.83	0.73	0.55
$-\ln Y_3(\text{Durham})$	lepton tag				1	0.67	0.59
$Y_3(\text{Jade})$	lifetime tag					1	0.65
$Y_3(\text{Durham})$	lifetime tag						1

Table 3: Correlation coefficients between the measurements of r^b.

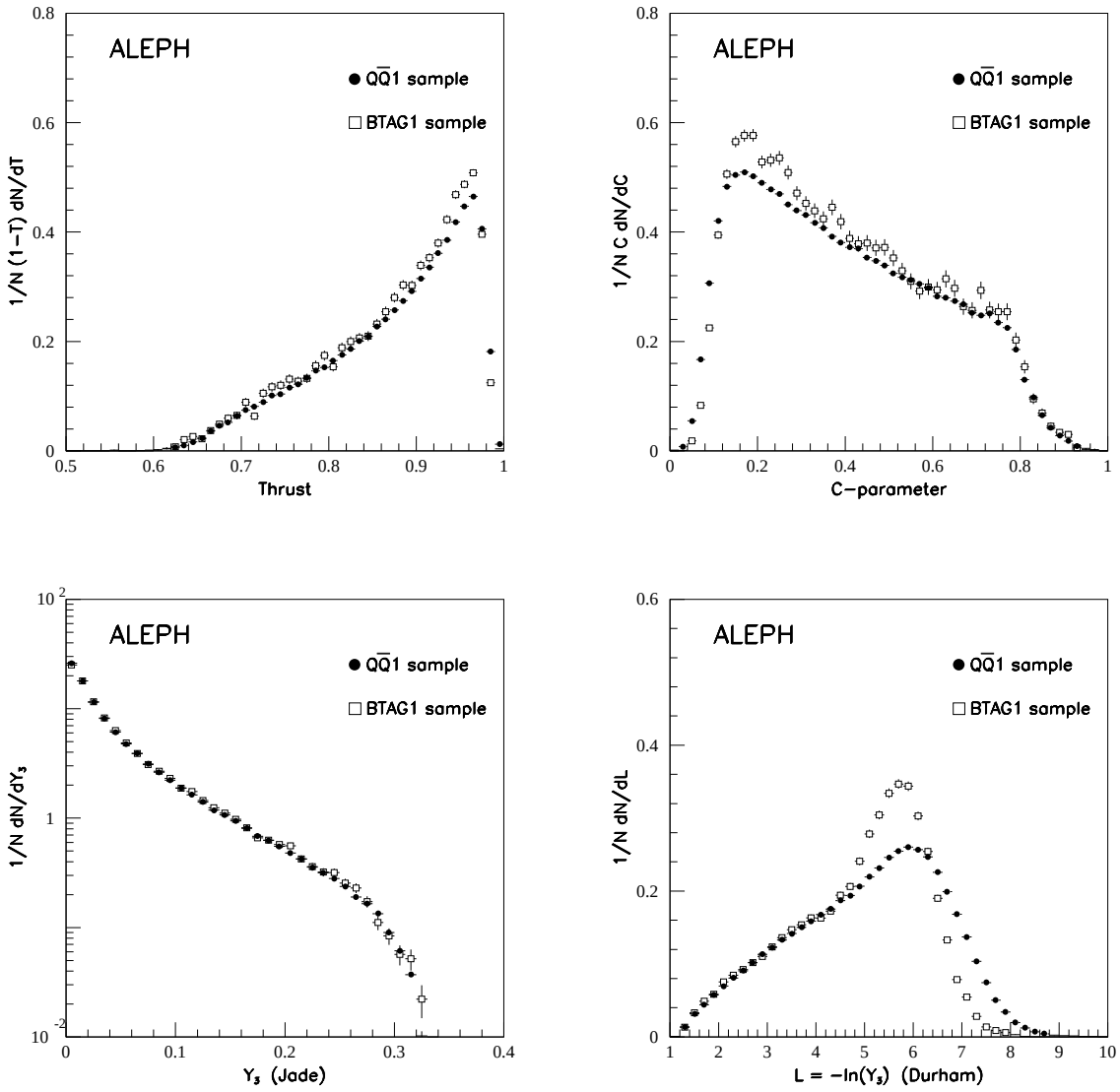

Figure 1: Normalized cross section of the full hadronic sample (full circles) and of the b-enriched sample (empty squares) selected with high-$p_\perp$ lepton tag.

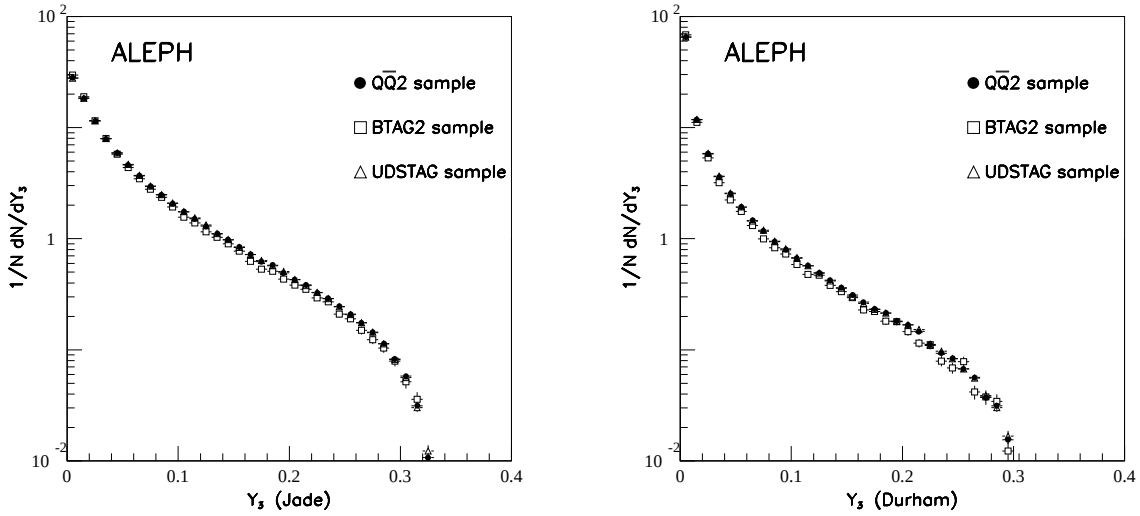

Figure 2: Normalized cross section of the full hadronic sample (full circles) of the b-enriched sample (empty squares) and of the light-quark-enriched sample (empty triangles) selected with lifetime tag.

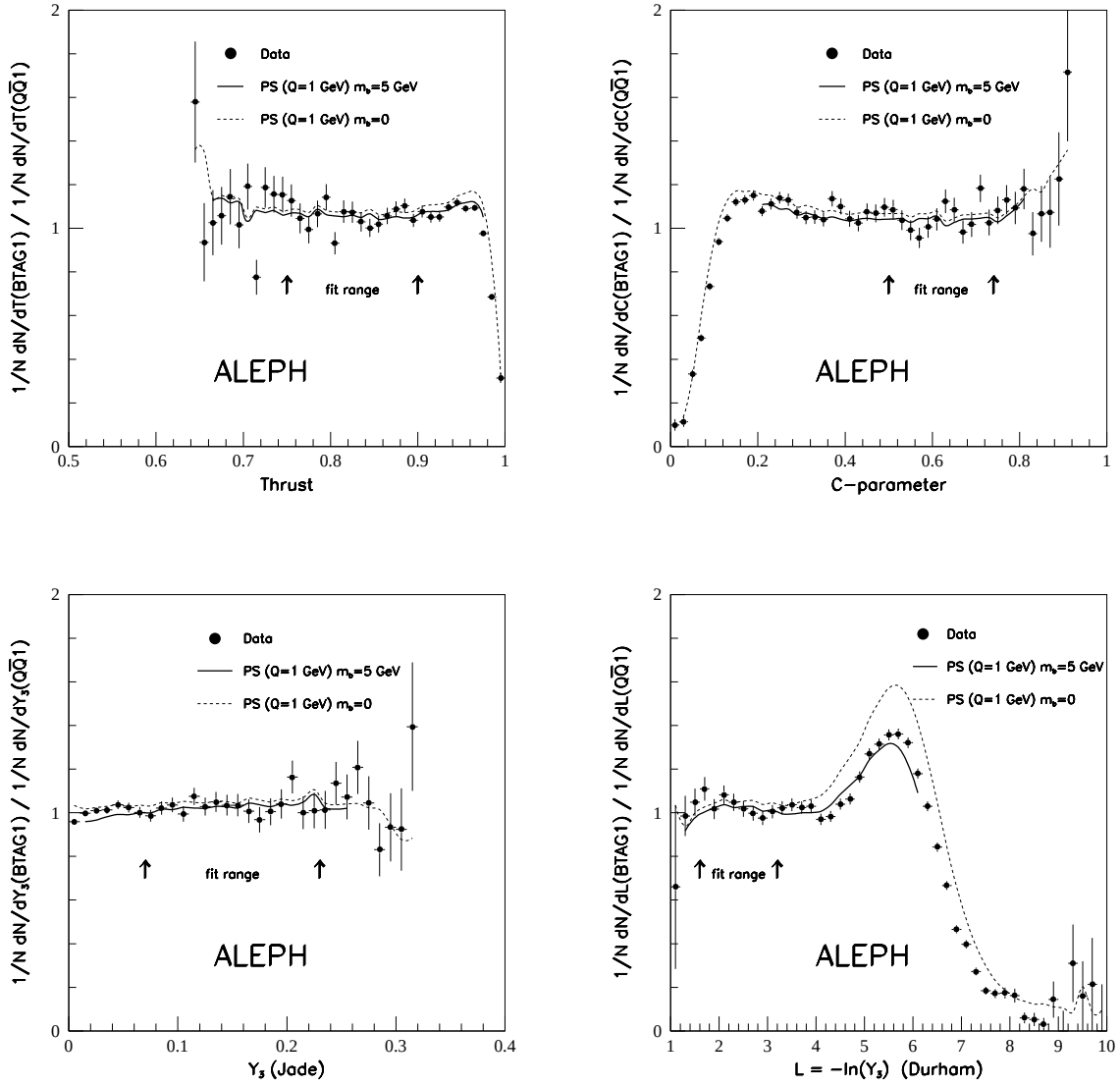

Figure 3: Ratio of the normalized cross section of the b-enriched sample tagged with high-$p_\perp$ lepton and the full hadronic sample. The full circles are the data, the solid line represents the fit result and the dashed line represents the theoretical prediction without the corrections for the finite mass of the b quark.

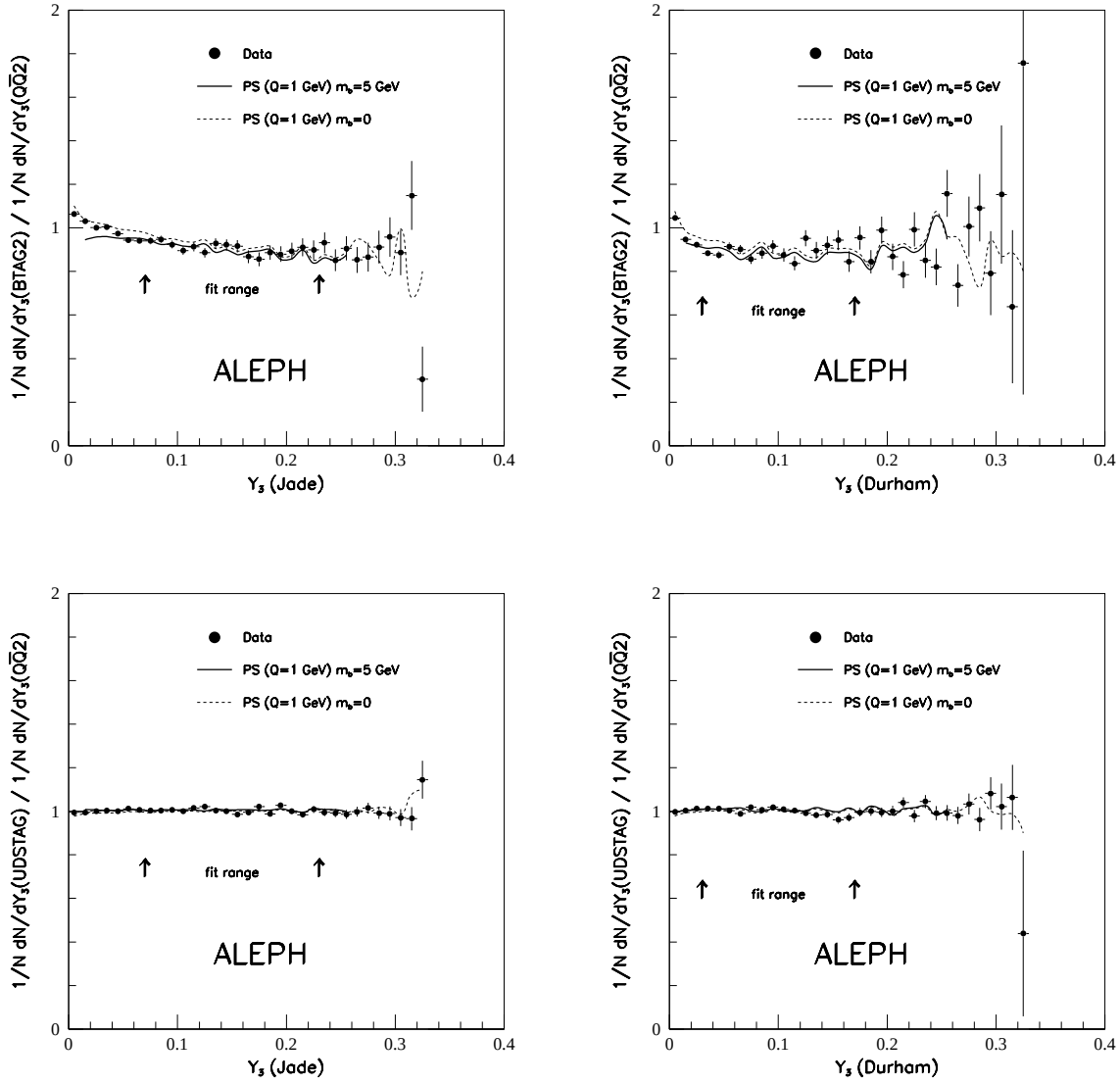

Figure 4: Ratio of the normalized cross section of the samples selected with lifetime tag and the full hadronic sample. The full circles are the data, the solid line represents the fit result and the dashed line the theoretical prediction without the corrections for the finite mass of the b quark.